Superfluidity of Bosons in Kagome Lattices with Frustration

Yi-Zhuang You, Zhu Chen, Xiao-Qi Sun, and Hui Zhai*

Institute for Advanced Study, Tsinghua University, Beijing 100084, China

(Received 7 August 2012; revised manuscript received 16 October 2012; published 28 December 2012)

In this Letter we consider spinless bosons in a kagome lattice with nearest-neighbor hopping and on-site interaction, and the sign of hopping is inverted by insetting a π flux in each triangle of the kagome lattice so that the lowest single particle band is perfectly flat. We show that in the high-density limit, despite the infinite degeneracy of the single particle ground states, interaction will select out the Bloch state at the K point of the Brillouin zone for boson condensation at the lowest temperature. As the temperature increases, the single-boson superfluid order can be easily destroyed, while an exotic triple-boson paired superfluid order will remain. We establish that this trion superfluid exists in a broad temperature regime until the temperature is increased to the same order of hopping and then the system turns into normal phases. Finally, we show that time-of-flight measurement of the momentum distribution and its noise correlation can be used to distinguish these three phases.

DOI: 10.1103/PhysRevLett.109.265302 PACS numbers: 67.85.Hj, 03.75.Lm

Flatband models have attracted considerable theoretical interest recently [1–13] because the single particle energies are degenerate inside the flatband; therefore, interactions play a dominant role in the many-body system and lead to many interesting quantum phases [7–13]. Among many different physical realizations of lattice models with flatband, a kagome lattice with only nearest neighbor hopping is perhaps one of the simplest. Recently, such a model has been realized experimentally using optical lattices by the Berkeley group [14]. However, the flatband in a normal kagome lattice is the highest band. By fast shaking the optical lattices, one can invert the sign of hopping, which has also been demonstrated experimentally for triangular optical lattices [15]. This technique can be applied straightforwardly to the kagome lattices. When the sign of hopping is inverted, it is equivalent to inserting a π flux in each triangle of the kagome lattice [16], and the flatband becomes the lowest band, as shown in Fig. 1.

In this Letter we consider spinless bosons with on-site interaction on the kagome lattice with sign-inverted hopping, such that the boson condensation is frustrated. Here we focus on the high-density superfluid (SF) regime, since those strongly correlated phases, such as the Mott insulator [7,8], the Wigner crystal [9], and the quantum Hall state [10,11], usually occur in the low-density regime. This high-density limit corresponds to a real system with a kagome optical lattice in the xy plane and weak confinement potential along the $\hat{z}$ direction. Therefore, each site is in fact a tube inside which bosons form a quasicondensate, and tunneling couples different tubes into a two-dimensional Josephson array described by a boson Hubbard model.

Here we shall discuss whether and how bosons can condense in the flatband, and what exotic type of superfluid occurs at finite temperature. The main findings are as follows.

(1) As the temperature increases, the system exhibits three different phases: a K-point ($\sqrt{3} \times \sqrt{3}$) superfluid phase, with bosons condensed to the single particle Bloch state at the momentum K point; an exotic "trion superfluid" phase, with triple-boson (quasi-)long-range order in the absence of single-boson ordering; and a normal phase of thermal boson gas without any order.

(2) The three phases are separated by two phase transitions at very different temperature scales. The higher one is of the hopping energy scale, while the lower one is 3 orders of magnitude smaller. Thus we predict a large temperature window in which the trion superfluid phase can be observed in experiments.

(3) We show that the time-of-flight (TOF) detection of momentum distribution can distinguish these three phases, and the third-order noise correlation provides a more direct evidence of the trion superfluid phase.

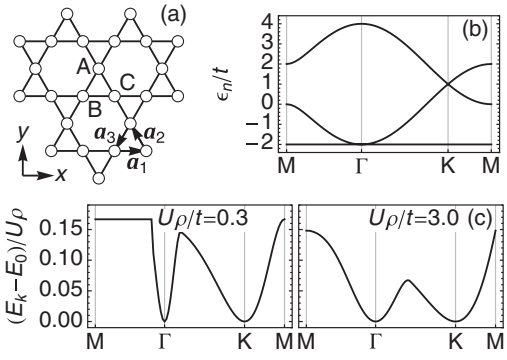

FIG. 1. (a) Kagome lattice, partitioned into A, B, C sublattices. (b) Band structure with inverted hopping sign, where $\Gamma = (0, 0)$, $K = (2\pi/3, 0)$, and $M = (\pi/2, \pi/2\sqrt{3})$. (c) Mean-field energy landscape for different $U\rho/t$. Energy shifted by $E_0 = -2t + U\rho/3$.

It has been a long-term effort to search for exotic bosonic state without single-boson superfluid order. In previous studies, two-boson paired superfluids (or charge-4e superconductor as paired Cooper pairs) have been proposed in various systems [17–25]. As far as we know, this is the first time that a triple-boson paired superfluid is proposed, and the underlying physics, i.e., the frustrated hopping in kagome geometry, is also different from that of previous examples. Moreover, unlike previous proposals where unconventional superfluids always take place at very low temperature, here the trion superfluid exists in a relatively high temperature regime, and, thus, it is easier for experimental realization. These results may also be generalized to interacting bosons in other flatband models with geometric frustration.

Band structure and mean-field.—The boson Hubbard model on the kagome lattice with π flux in each triangle is given by $\hat{H} = \hat{H}_t + \hat{H}_U$, with the hopping term $\hat{H}_t = t\sum_{\langle ij\rangle}\hat{b}_i^\dagger \hat{b}_j + \text{H.c.}$, and the interaction term $\hat{H}_U = U\sum_i \hat{n}_i(\hat{n}_i - 1) - \mu\sum_i \hat{n}_i$, where $\hat{n}_i = \hat{b}_i^\dagger \hat{b}_i$. Here t is positive [16]. In the momentum space, the hopping Hamiltonian reads $\hat{H}_t = \sum_{\boldsymbol{k}} \hat{b}_{\boldsymbol{k}}^\dagger h(\boldsymbol{k}) \hat{b}_{\boldsymbol{k}}$ with $\hat{b}_{\boldsymbol{k}} = (\hat{b}_{\boldsymbol{k}A}, \hat{b}_{\boldsymbol{k}B}, \hat{b}_{\boldsymbol{k}C})^\mathsf{T}$ and

$$h(\boldsymbol{k}) = 2t\begin{pmatrix} 0 & \cos k_3 & \cos k_2 \\ \cos k_3 & 0 & \cos k_1 \\ \cos k_2 & \cos k_1 & 0 \end{pmatrix}, \tag{1}$$

where $k_i \equiv \boldsymbol{k}\cdot\boldsymbol{a}_i$, and $\boldsymbol{a}_1 = (1, 0)$, $\boldsymbol{a}_2 = (-\frac{1}{2}, \frac{\sqrt{3}}{2})$, $\boldsymbol{a}_3 = (-\frac{1}{2}, -\frac{\sqrt{3}}{2})$ as shown in Fig. 1(a). Its lowest band is perfectly flat with a quadratic band touching at the Γ point, as shown in Fig. 1(b).

Because of the infinite degeneracy of the single particle ground state, free bosons cannot condense. At the mean-field level, we first consider the single particle state with translational symmetry labeled by momentum $\boldsymbol{k}$. Taking the mean-field ansatz $\langle \hat{b}_{\boldsymbol{k}}\rangle = z \equiv (z_A, z_B, z_C)^\mathsf{T}$ with the normalization condition $z^\dagger z = \rho$, where ρ is the boson filling per unit cell, we can minimize the mean-field energy function $E_{\boldsymbol{k}}[z] = z^\dagger h(\boldsymbol{k}) z + U(|z_A|^4 + |z_B|^4 + |z_C|^4)$ with respect to z, and denote the optimal energy as $E_{\boldsymbol{k}} = \min_z E_{\boldsymbol{k}}[z]$. This mean-field energy landscape in Fig. 1(c) shows that the single particle degeneracy is lifted by the Hartree energy. Γ and K points are selected out to be the energy minimum. This is because inside the flatband, the single particle wave functions have equal amplitudes among the three sublattices only at Γ and K points, and their uniform densities are favored by the repulsive interaction.

The Bloch wave functions for Γ and K points are determined by minimizing the mean-field energy,

$$\begin{aligned} \psi_\Gamma(\boldsymbol{r}_i) &= \frac{1}{\sqrt{3}}(1, e^{\pm 2\pi i/3}, e^{\mp 2\pi i/3})^\mathsf{T}, \\ \psi_K(\boldsymbol{r}_i) &= \frac{1}{\sqrt{3}} e^{i\boldsymbol{k}_K\cdot\boldsymbol{r}_i}(1, -1, -1)^\mathsf{T}, \end{aligned} \tag{2}$$

with $\boldsymbol{k}_K = (2\pi/3, 0)$. In real space, both two wave functions satisfy two conditions: (i) their densities are uniform, which minimize the mean-field interaction energy, and (ii) their phases follow the "3-color arrangement," meaning that each pair of two neighboring sites takes different phases out of 1, $e^{2\pi i/3}$ and $e^{-2\pi i/3}$, as depicted in Fig. 2, such that the kinetic energy is also minimized. The mean-field energy is minimized to $E_0 = -2t + U\rho/3$, as long as both conditions (i) and (ii) are satisfied, while the translation invariance is not a necessary condition and can be released. Then one can find extensive numbers of state without translation invariance but satisfying both (i) and (ii), as exemplified in Figs. 2(c) and 2(d).

Quantum fluctuation and order from disorder.—The extensive number of degenerate mean-field states can be further lifted by quantum fluctuations, because the zero-point energy (ZPE) of Bogoliubov phonons is different for different mean-field states. For a given mean-field configuration $\langle \hat{b}_i\rangle = \sqrt{\rho}e^{i\theta_i}$, its Bogoliubov Hamiltonian is

$$\begin{aligned} H[\theta_i] = {} & t\sum_{\langle ij\rangle}(\hat{b}_i^\dagger \hat{b}_j + \text{H.c.}) - \mu\sum_i \hat{b}_i^\dagger \hat{b}_i \\ & + U\rho\sum_i (2\hat{b}_i^\dagger \hat{b}_i + e^{2i\theta_i}\hat{b}_i^\dagger \hat{b}_i^\dagger + \text{H.c.}), \end{aligned} \tag{3}$$

where $\mu = -2t + 2U\rho/3$. Diagonalization of $H[\theta_i]$ leads to $H[\theta_i] = \sum_m \omega_m[\theta_i](\hat{\gamma}_m^\dagger \hat{\gamma}_m + 1/2)$, with $\hat{\gamma}_m$ being a Bogoliubov boson operator. Thus the ZPE associated

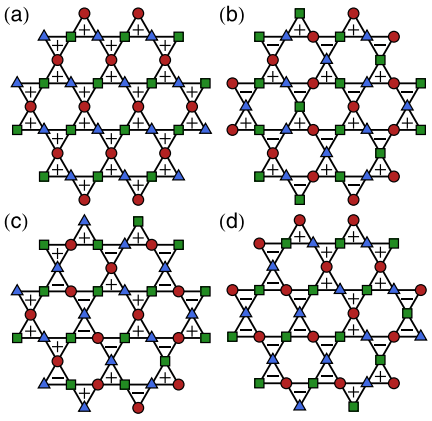

FIG. 2 (color online). (a), (b) Phase configurations of the condensates at the Γ point (a) and the K point (b), (c), (d) random 3-color arrangement. Phase θ_i is denoted by colors: red circle $= 0$, green square $= 2\pi i/3$, blue triangle $= -2\pi i/3$. "$\pm$" mark out the vorticity around each triangle. (a) ψ_Γ is a "vorticity ferromagnetic" state and (b) ψ_K is a "vorticity antiferromagnetic" state.

with this given $\{\theta_i\}$ configuration equals to $\Lambda[\theta_i] = \frac{1}{2}\sum_m \omega_m[\theta_i]$ by setting $\hat{\gamma}_m^\dagger \hat{\gamma}_m = 0$.

For condensates at the Γ and K points, the Bogoliubov excitations have quantum number $\boldsymbol{k}$ and they have well-defined dispersion, as shown in Fig. 3(a). One finds that the sound velocity c of the K-point condensate is smaller that that of the Γ-point condensate; hence, the K-point condensate as a lower ZPE, as $\Lambda \sim c^2$. This is also evidenced from the mean-field energy landscape, as shown in Fig. 1(c), where the energy landscape changes less rapidly near the K point than that near the Γ point, indicating softer Goldstone mode and lower ZPE.

For a generic mean-field state in the degenerate manifold, the Bogoliubov spectrum has no well-defined dispersion because of the absence of translation symmetry. Here we randomly sample 4000 configurations on a 240-site kagome lattice with uniform density and satisfying the 3-color arrangement, and then we calculate their ZPEs numerically. We find that their ZPEs all rest between the Γ-point condensate and the K-point condensate, i.e., $\forall\{\theta_i\}$: $\Lambda[K] \le \Lambda[\theta_i] \le \Lambda[\Gamma]$, as seen from Fig. 3(b). So the degeneracy can be completely removed via the order-by-disorder mechanism. At sufficiently low temperature, bosons will condense to the K point (or its symmetry related points).

Thermal fluctuation and phase diagram.—Because all the ZPEs are in the range from $\Lambda[K]$ to $\Lambda[\Gamma]$, it is natural to introduce the energy scale for zero-point fluctuation as $J = \Lambda[\Gamma] - \Lambda[K]$. Beyond this energy scale, the condensation at the K point will be destroyed. As shown in Fig. 3(c), J will vanish in both the small and large U limit. The asymptotic behavior goes like $J \propto U\rho$ for $U\rho \ll t$ and $J \propto t^{3/2}(U\rho)^{-1/2}$ for $U\rho \gg t$. The maximum of J is achieved around $U\rho/t = 3$. It is remarkable to find that even the maximum value of J is 3 orders of magnitude smaller than t. It is still quite challenging to reach such a low temperature in current cold atom experiments.

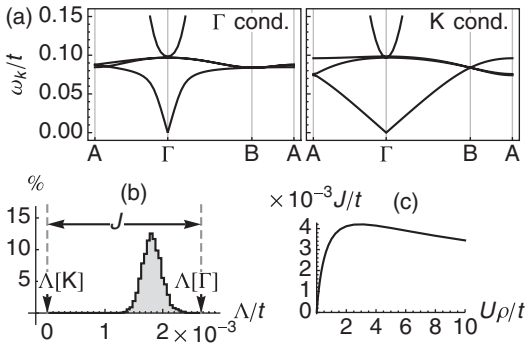

FIG. 3. (a) Bogoliubov spectra for Γ-point (left) and K-point (right) condensates at $U\rho/t = 0.3$. Momentum points are defined as $A = (\pi/3, 0)$ and $B = (\pi/3, \pi/3\sqrt{3})$. (b) Distribution of the zero-point energy (ZPE) Λ of the degenerate mean-field configurations. Two dashed lines denote the ZPE for K- and Γ-point condensates. The vertical axis is the probability for the particular ZPE. (c) J/t vs $U\rho/t$ plot.

However, the conventional Bose condensate at the lowest temperature is not the most interesting phase. The most interesting phase in this system exists at the temperature regime $k_B T > J$. In this regime, the system will enter a thermal mixed state in which all mean-field configurations satisfying conditions (i) and (ii) mentioned above are almost equally populated. In this thermal mixed state, for each site the condensate phase can take $\theta_i = 0, \pm 2\pi/3$ with equal probabilities. Thus, the single boson correlation will become short ranged, i.e., $\langle \hat{b}_i^\dagger \hat{b}_j \rangle = \rho_s \langle e^{-i\theta_i} e^{i\theta_j} \rangle \to 0$. However, as long as the 3-color arrangement is satisfied, at every site $e^{3i\theta_i} \equiv 1$ always holds. Thus, the triple-bosons operator can still possess long-range correlation; i.e., $\langle \hat{b}_i^{\dagger 3} \hat{b}_j^3 \rangle = \rho_s^3 \langle e^{-3i\theta_i} e^{3i\theta_j} \rangle \to \rho_s^3$ [26]. This trion SF supports many interesting properties, such as $1/3$ fractionalized vortices, which will be studied in the future.

Since the 3-color arrangement is enforced by the kinetic energy, bosons will condense in triples as long as $T < t$. When T is increased to $\sim t$, the long wavelength fluctuation of the $U(1)$ phase will lead to a Kosterlitz-Thouless phase transition from the trion SF to the normal state. This transition temperature can be estimated from the superfluid stiffness, which can be calculated from the free-energy response to the phase twist. Let $b_i = w_i e^{i\theta_i} e^{i\boldsymbol{q}\cdot\boldsymbol{r}_i}$, where $e^{i\boldsymbol{q}\cdot\boldsymbol{r}_i}$ is the applied phase twist. In the temperature regime $T \gg J$, we can ignore the zero-point energy, and the energy functional for a given $\{\theta_i\}$ configuration reads $E_{\boldsymbol{q}}[\theta_i, w_i] = t\sum_{\langle ij\rangle}(w_i^* w_j e^{-i(\theta_i-\theta_j)} e^{-i\boldsymbol{q}\cdot(\boldsymbol{r}_i-\boldsymbol{r}_j)} + \text{H.c.}) + U\sum_i |w_i|^4$, and because all the configurations must be taken into account under thermal average, the averaged energy functional reads

$$\mathcal{E}_{\boldsymbol{q}}[w_i] = \sum_{\{\theta_i\}} E_{\boldsymbol{q}}[\theta_i, w_i] = -\frac{t}{2}\sum_{\langle ij\rangle}(w_i^* w_j e^{-i\boldsymbol{q}\cdot(\boldsymbol{r}_i-\boldsymbol{r}_j)} + \text{H.c.}) + U\sum_i |w_i|^4. \tag{4}$$

It is interesting to note that Eq. (4) is the same as a mean-field energy of bosons in the kagome lattice *without* frustration, because the sign of hopping is now inverted back. Mathematically, it is because taking thermal averages leads to $\langle e^{i(\theta_i-\theta_j)} \rangle = -1/2$. Since the kinetic energy frustration is released, trion SF will have a finite stiffness. It can be obtained by minimizing $\mathcal{E}_{\boldsymbol{q}}[w_i]$ with respect to w_i and expanding the optimal energy in terms of small $\boldsymbol{q}$, which leads to $\min_{\{w_i\}}\mathcal{E}_{\boldsymbol{q}}[w_i] \simeq -2t + \frac{U\rho}{3} + \frac{1}{2}t\boldsymbol{q}^2$. Therefore, the stiffness is t, which gives an estimate of the Kosterlitz-Thouless transition temperature as $T_{\text{KT}} = t/\pi$. For Rb atoms, t is around 15 nK with a moderate lattice depth, and thus T_{KT} is a few nK.

With the analysis above, we reach the phase diagram as shown in Fig. 4(a). In Fig. 4(b), we

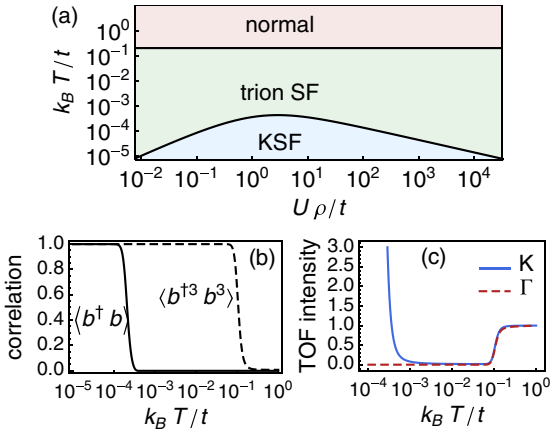

FIG. 4 (color online). (a) Phase diagram. It contains three phases: the conventional superfluid phase with boson condensation at the K point (KSF), trion superfluid (trion SF) phase, and the normal phase. (b) The long-range correlation for $\langle \hat{b}_i^\dagger \hat{b}_j \rangle$ and $\langle \hat{b}_i^{\dagger 3} \hat{b}_j^3 \rangle$ as a function of temperature $k_B T/t$. (c) TOF intensity at the Γ and the K point as a function of temperature $k_B T/t$. (b) and (c) are calculated at $U\rho/t = 1$.

show the one-boson and three-boson correlation function as a function of temperature for a fixed $U\rho/t$. The one-particle correlation $\langle \hat{b}_i^\dagger \hat{b}_j \rangle$ is calculated as $\rho_s \sum_{\{\theta_i\}} e^{-i(\theta_i-\theta_j)} e^{-\Lambda[\theta_i]/T}$, where the configuration summation can be restricted in the 3-color arrangement patterns, since other configurations cost energy of the order t and their contribution is negligible at low temperature around the order J. While on the other hand, when we calculate the three-boson correlation $\langle \hat{b}_i^{\dagger 3} \hat{b}_j^3 \rangle = \rho_s^3 \sum_{\{\theta_i\}} e^{-3i(\theta_i-\theta_j)} e^{-E[\theta_i]/T}$, the summation goes over all configurations $\{\theta_i\}$, and the energy is given by $E[\theta_i] = 2t \sum_{\langle ij \rangle} \cos(\theta_i - \theta_j)$, where we have ignored the ZPE as it is negligible compared to $E[\theta_i]$. Figure 4(b) shows that there indeed exists a large temperature window where the one-boson correlation function vanishes while the three-boson correlation function remains finite.

Detection.—Finally, we show that the difference between these three phases can be detected by a straightforward measurement of momentum distribution via a TOF image [27]. When bosons condense into K points of the Brillouin zone, a TOF image will display sharp Bragg peaks at K points (or its equivalent K' points) in the reciprocal lattice, as shown in Fig. 5(a). Moreover, due to the interference effect from the phase structure satisfying the 3-color arrangement, it is easy to show that the strongest peaks do not appear in the first Brillouin zone, but instead at its reciprocal lattice vector points in the second Brillouin zone. As temperature increases to the trion SF phase, all the 3-color arrangements are thermally mixed, and the Bragg peak at the K point disappears as the single-boson superfluid order vanishes. However, in contrast to the normal state, the TOF image displays nontrivial features as shown in Fig. 5(b). A large honeycomb structure appears, and the hexagon is 4 times the area of the first

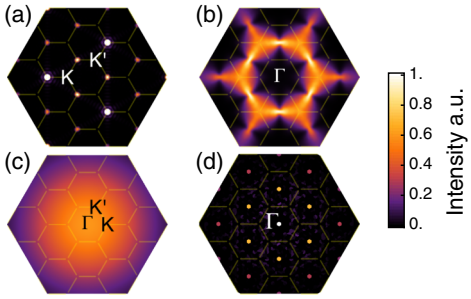

FIG. 5 (color online). (a)–(c) TOF image of momentum distribution for three phases. (a) KSF, (b) trion SF, (c) normal. The thin lines of the honeycomb trace out the Brillouin zone boundary. For (b) and (c), the image is averaged over many times of TOF experiments. (d) Profile of $C(\boldsymbol{k})$ simulated in the trion SF phase by analyzing the noise correlation among 100 TOF images.

Brillouin zone, and the intensity at the Γ point is always zero, because the zero-momentum component of the Fourier transformation is exactly cancelled out due to the 3-color arrangement. At the highest temperature normal state, the TOF image becomes a featureless Gaussian and the intensity at the Γ point becomes the maximum, as shown in Fig. 5(c). Thus, we predict that the intensity at the K point rapidly decreases at the transition from K-point condensate to trion SF, and the intensity of the Γ point rapidly increases at the transition from trion SF to normal state, as shown in Fig. 4(c).

In addition, the trion SF order can also be probed by analyzing the three-point noise correlation of the TOF images. This requires repeating the TOF experiment many times to obtain the noise signal $\delta n_{\boldsymbol{k}} = n_{\boldsymbol{k}} - \langle n_{\boldsymbol{k}} \rangle$ for each image, as shown in Fig. 5(b) [28,29]. We propose that the triple-boson long-range correlation can be observed from the three-point noise correlation $C(\boldsymbol{k}) = \sum_{\boldsymbol{k}_1+\boldsymbol{k}_2+\boldsymbol{k}_3=\boldsymbol{k}} \langle \delta n_{\boldsymbol{k}_1} \delta n_{\boldsymbol{k}_2} \delta n_{\boldsymbol{k}_3} \rangle$, where it is important to collect information from all the points satisfying $\boldsymbol{k}_1 + \boldsymbol{k}_2 + \boldsymbol{k}_3 = \boldsymbol{k}$ into $C(\boldsymbol{k})$. It is straightforward to show that this noise correlation displays sharp feature only in the trion SF phase, and the triple-boson correlation is directly related to the noise correlation via $\langle \hat{b}_i^{\dagger 3} \hat{b}_j^3 \rangle \propto \sum_{\boldsymbol{k}_{1,2,3}} \langle \delta n_{\boldsymbol{k}_1} \delta n_{\boldsymbol{k}_2} \delta n_{\boldsymbol{k}_3} \rangle \times e^{-i(\boldsymbol{k}_1+\boldsymbol{k}_2+\boldsymbol{k}_3)(\boldsymbol{r}_i-\boldsymbol{r}_j)}$. Therefore, $C(\boldsymbol{k})$ shows sharp peaks at Γ points in the trion SF phase, as in Fig. 5(d), providing direct evidence for the long-range correlation of $\langle \hat{b}_i^{\dagger 3} \hat{b}_j^3 \rangle$.

We would like to thank T.-L. Ho and H. Yao for helpful discussions. This work is supported by Tsinghua University Initiative Scientific Research Program, NSFC Grants No. 11004118 and No. 11174176, and NKBRSFC under Grant No. 2011CB921500.

*hzhai@tsinghua.edu.cn

[1] S. D. Huber and E. Altman, Phys. Rev. B **82**, 184502 (2010).
[2] S. Endo, T. Oka, and H. Aoki, Phys. Rev. B **81**, 113104 (2010).

[3] E. Tang, J.-W. Mei, and X.-G. Wen, Phys. Rev. Lett. **106**, 236802 (2011).
[4] K. Sun, Z.-C. Gu, H. Katsura, and S. Das Sarma, Phys. Rev. Lett. **106**, 236803 (2011).
[5] T. Neupert, L. Santos, C. Chamon, and C. Mudry, Phys. Rev. Lett. **106**, 236804 (2011).
[6] F. Wang and Y. Ran, Phys. Rev. B **84**, 241103(R) (2011).
[7] S. A. Parameswaran, I. Kimchi, A. M. Turner, D. M. Stamper-Kurn, and A. Vishwanath, arXiv:1206.1072v1.
[8] I. Kimchi, S. A. Parameswaran, A. M. Turner, and A. Vishwanath, arXiv:1207.0498v1.
[9] C. Wu, D. Bergman, L. Balents, and S. Das Sarma, Phys. Rev. Lett. **99**, 070401 (2007).
[10] Y.-F. Wang, H. Yao, Z.-C. Gu, C.-D. Gong, and D. N. Sheng, Phys. Rev. Lett. **108**, 126805 (2012).
[11] Y.-F. Wang, H. Yao, C.-D. Gong, and D. N. Sheng, Phys. Rev. B **86**, 201101(R) (2012).
[12] G. Möller and N. R. Cooper, Phys. Rev. Lett. **108**, 045306 (2012).
[13] X.-H. Zhang and S.-P. Kou, arXiv:1205.6641.
[14] G.-B. Jo, J. Guzman, C. K. Thomas, P. Hosur, A. Vishwanath, and D. M. Stamper-Kurn, Phys. Rev. Lett. **108**, 045305 (2012).
[15] J. Struck, C. Ölschläger, R. Le Targat, P. Soltan-Panahi, A. Eckardt, M. Lewenstein, P. Windpassinger, and K. Sengstock, Science **333**, 996 (2011).
[16] This is gauge equivalent to the situation that one of the three hopping signs (from A site to B site, from B site to C site, or from C site to A site) is inverted, and such a situation may be easier for experimental implementation.
[17] E. Berg, E. Fradkin, and S. A. Kivelson, Nat. Phys. **5**, 830 (2009).
[18] L. Radzihovsky and A. Vishwanath, Phys. Rev. Lett. **103**, 010404 (2009).
[19] L. Radzihovsky, Phys. Rev. A **84**, 023611 (2011).
[20] D. F. Agterberg and H. Tsunetsugu, Nat. Phys. **4**, 639 (2008).
[21] F. Zhou, Phys. Rev. Lett. **87**, 080401 (2001).
[22] S. Mukerjee, C. Xu, and J. E. Moore, Phys. Rev. Lett. **97**, 120406 (2006).
[23] D. Podolsky, S. Chandrasekharan, and A. Vishwanath, Phys. Rev. B **80**, 214513 (2009).
[24] A. J. A. James and A. Lamacraft, Phys. Rev. Lett. **106**, 140402 (2011).
[25] C.-M. Jian and H. Zhai, Phys. Rev. B **84**, 060508(R) (2011).
[26] A similar argument has been presented in the spin model; see D. A. Huse and A. D. Rutenberg, Phys. Rev. B **45**, 7536 (1992).
[27] For the case of flipping the hopping sign along only one type of bounds its TOF image will be shifted by one reciprocal lattice vector.
[28] E. Altman, E. Demler, and M. D. Lukin, Phys. Rev. A **70**, 013603 (2004).
[29] S. Flling, F. Gerbier, A. Widera, O. Mandel, T. Gericke, and I. Bloch, Nature (London) **434**, 481 (2005).